

Magnetism in Nickel and Synchrotron Beam Polarization Studied by X-ray Diffraction

D. Laundy,^{a,b}† S. Brown,^{a,c} M. J. Cooper,^{a,b*} D. Bowyer,^{a,d} P. Thompson,^{a,b} D. F. Paul^{a,b} and W. G. Stirling^{a,c}

^aXMaS CRG, ESRF, 38043 Grenoble CEDEX, France, ^bDepartment of Physics, University of Warwick, Coventry CV4 7AL, UK, ^cDepartment of Physics, University of Liverpool, Liverpool L69 7ZE, UK, and ^dDepartment of Physics, University of Keele, Keele, Staffs ST5 5BG, UK. E-mail: csmc@spec.warwick.ac.uk

(Received 9 December 1997; accepted 15 December 1997)

The ratio of the magnetic to the charge form factors of nickel has been determined by white-beam X-ray diffraction. The measurements were made on the new UK magnetic scattering beamline (XMaS) on a dipole source at the ESRF. The data comprise the three $(h,h,0)$ reflections (4,4,0), (6,6,0) and (8,8,0) and the seven high-order $(h,0,0)$ reflections (6,0,0) to (18,0,0), which doubles the range of wavevectors compared to previous studies. The data have been analysed using Hartree–Fock free-ion wave functions and core electron polarization effects were included. The results support the interpretation of neutron data obtained at lower momentum transfer for the e_g and t_{2g} orbital occupancies. The polarization of the dipole source is deduced to vary from 99.88 to 99.83% between 5 and 15 keV, respectively. This high value makes it an extremely suitable source for studies of ferromagnetism.

Keywords: ferromagnetism; circular polarization; magnetic form factors.

1. Introduction

As explained below, the degree of polarization of the source is a critical parameter in studies of ferromagnetism. It has been measured in the present study of 3d magnetism in ferromagnetic nickel using a white-beam technique, which extends the measurements of magnetic form factors to higher momentum transfer than any reported in previous neutron or X-ray investigations using X-ray techniques.

The magnetism of the 3d transition metals is thought to be well described by a band model with the exchange interaction causing a difference in the occupancy of the 3d sub-bands. In nickel this leads to a magnetic moment of $0.57 \mu_B$ per atom at room temperature. There is evidence from polarized neutron measurements three decades ago (Mook, 1966) to support this picture and also to suggest that there is some negative spin polarization of the 4s band. Those neutron measurements were also able to determine that there was a deviation from spherical symmetry caused by crystal field effects on the charge density of the spin-polarized 3d electrons. The pioneering neutron experiments on iron (Shull & Yamada, 1962) and nickel (Mook, 1966) could only be matched by complementary X-ray experiments after the advent of second-generation synchrotron sources which provided high-intensity highly polarized and stable beams of X-rays. The first X-ray form-

factor measurements were made at the Synchrotron Radiation Source, Daresbury Laboratory, on iron (Laundy *et al.*, 1991; Collins *et al.*, 1992) and nickel (Zukowski *et al.*, 1992).

As discussed below, measurements of this type will yield better results if performed at a low-emittance third-generation source capable of producing highly polarized X-rays, such as the European Synchrotron Radiation Facility (ESRF). The improvement in the polarization of the radiation is a direct consequence of the reduction in the size of the electron beam. The polarization of the X-rays on a second-generation machine is typically 97.0% for a dipole-magnet source, which is much lower than the value reported below for the XMaS beamline at the ESRF. Another advantage of a third-generation source such as the ESRF is the larger critical energy of the X-ray spectrum, which allows higher-order reflections to be studied by the white-beam method. With these advantages in mind, measurements have been made on the XMaS beamline, a new dipole beamline at the ESRF dedicated to magnetic and high-resolution diffraction and operated jointly by the Universities of Liverpool and Warwick for the UK scientific community.

1.1. Principles of the white-beam method

The theory of the scattering of X-rays is given, for example, by Blume (1985) and Lovesey (1987) and detailed in the book by Lovesey & Collins (1996). The strongest

† Now at Daresbury Laboratory, CLRC, Warrington WA4 4AD, UK.

mechanism for coherent scattering of X-rays from bound electrons is Thomson scattering from the electron charge density, $\rho(\mathbf{r})$. The scattering amplitude for a reflection with scattering vector \mathbf{K} is proportional to the form factor, $f(\mathbf{K})$, which is given by the formula

$$f(\mathbf{K}) = \int \rho(\mathbf{r}) \exp(-i\mathbf{K}\cdot\mathbf{r}) d^3\mathbf{r}. \quad (1)$$

The magnetic scattering amplitude, which is determined by the interaction between the electronic spin and orbital moments and the electromagnetic field of the X-rays, is weaker than Thomson scattering by a factor E_X/mc^2 , where E_X is the energy of the diffracted photons and mc^2 is the rest energy of the electron (512 keV). Furthermore, only a small fraction of the electrons have unpaired spins. The magnetic scattered amplitude is proportional to the magnetic form factor $f^{\text{mag}}(\mathbf{K})$, the Fourier transform of the charge density, $m(\mathbf{r})$, of the electrons with unpaired moments,

$$f^{\text{mag}}(\mathbf{K}) = \int m(\mathbf{r}) \exp(-i\mathbf{K}\cdot\mathbf{r}) d^3\mathbf{r}. \quad (2)$$

The nature of the interaction is such that the magnetic amplitude is phase shifted by $\pi/2$ compared with the Thomson amplitude. In ferromagnetic nickel the charge and magnetic lattices are identical and so the two types of reflection are coincident. Thus, by using an incident beam with complex (circular) polarization, there is coupling between the Thomson and the magnetic amplitudes. The measured intensity is then first order in the weak magnetic

amplitude and the magnetic signal can be isolated from the charge signal by reversing the moment direction in the sample using an applied magnetic field to change the sign of the cross term.

The experimental geometry is chosen to maximize the ratio of the magnetically modulated term to the Thomson intensity (see, for example, Zukowski *et al.*, 1992). The sample is aligned to diffract through 90° in a horizontal plane to take advantage of the polarization dependence of the Thomson scattering and the linear polarization of the synchrotron radiation in the orbital plane of the storage ring, *i.e.* to diminish the charge scattering. The incident beam is not precisely in the orbital plane but at a small angle above or below it in order that the beam contains both linearly and circularly polarized components. The moments are oriented by an applied magnetic field parallel to the scattered beam. If I_+ and I_- are the measured intensities for the field applied first parallel and then anti-parallel to the scattered beam, the X-ray 'flipping ratio', R , is defined as

$$R = (I_+ - I_-)/(I_+ + I_-), \quad (3)$$

and in this geometry it is related to the charge $f(\mathbf{K})$ and magnetic form factors $f^{\text{mag}}(\mathbf{K})$ (Laundy *et al.*, 1991) by the equation

$$R = (E_X/mc^2)[P_C/(1 - P_L)] f^{\text{mag}}(\mathbf{K})/f(\mathbf{K}), \quad (4)$$

where P_C and P_L are the degrees of circular and linear polarization, respectively, of the incident X-ray beam. The ratio R depends on the polarization of the incident beam through the factor $f_P = P_C/(1 - P_L)$. The polarization of the synchrotron radiation varies with the take-off angle, φ , above or below the orbital plane. By varying φ the factor f_P can be maximized. Fig. 1 shows P_C , P_L and f_P , plotted as a function of φ , as deduced from the analysis described below. The optimum take-off angle for the XMaS dipole magnet beamline, D28, at the ESRF is seen to be $\varphi \simeq 3 \mu\text{rad}$, which corresponds to a height at the sample position, 25 m from the source, of only approximately $100 \mu\text{m}$ above or below the beam centre.

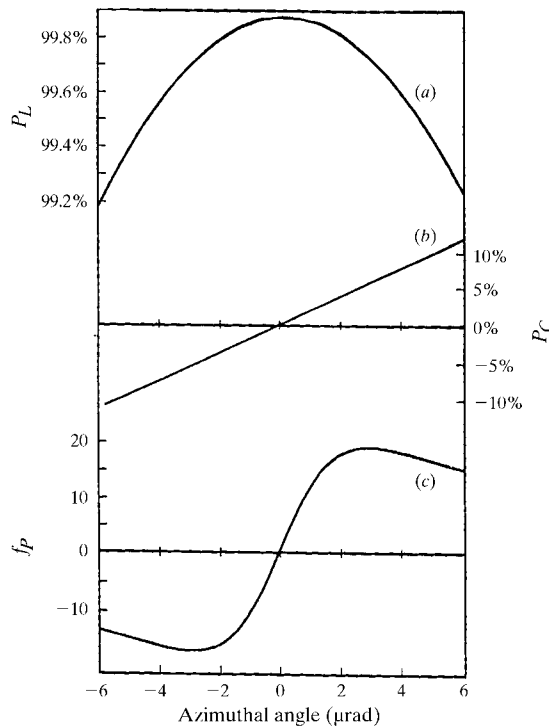


Figure 1

(a) The linear polarization, P_L , calculated from measurements made on the XMaS beamline; (b) circular polarization, P_C ; (c) the factor $f_P = P_C/(1 - P_L)$, which enhances the ratio of magnetic to charge scattering in the white-beam diffraction method.

2. Experimental details

The experimental method follows that of previous experiments (Laundy *et al.*, 1991; Collins *et al.*, 1992; Zukowski *et al.*, 1992). The fact that the Bragg angle is fixed ($2\theta_B = 90^\circ$ in the horizontal diffraction plane) means that white beam must be used. An intrinsic germanium semiconductor detector with sufficient resolution (~ 200 eV at 6 keV, ~ 400 eV at 60 keV) to separate the Bragg peaks from each other and from fluorescence lines was used. The sample was a single crystal of nickel with dimensions $3 \times 3 \times 4$ mm with four (110) and two (100) polished rectangular faces. It was mounted on a goniometer which, in turn, sat on a rotary table. The sample was aligned by taking Laue photographs of the required reflection in back reflection

and then rotated horizontally through 45° to set the scattering angle to 90° . The output from the detector was amplified and fed into an analogue-to-digital converter and then to a multichannel analyser. An electromagnet with a hole bored through one of the poles provided a 0.4 T field to magnetize the sample in the direction of the diffracted beam. The magnetic field was reversed under computer control following an asynchronous cycle with a basic period of 1 s. During each period the data from the detector were accumulated and stored separately for each of the reflection orders being studied.

The experiment was set up in the optics hutch of the XMaS beamline. The X-ray energy range available for the experiment was determined by the critical energy of the dipole source, which is 9 keV. In order to take advantage of the high beam polarization it was necessary to locate the beam centre accurately and then to translate the apparatus a known distance above or below the beam centre. It was also necessary to know the linear and circular polarization of the beam at the chosen position. To this end the entire apparatus was mounted on a table with a motorized vertical translation. The beam centre was determined by scanning the apparatus vertically through a range of approximately $-250 \mu\text{m}$ to $+250 \mu\text{m}$ about the beam centre and measuring the diffracted intensities, the minimum corresponding to the orbital plane. The variation of intensity with the azimuthal angle allowed the electron beam source to be characterized so that the X-ray polarization could be calculated. The multichannel analyser recorded the reflection set $(h,h,0)$ or $(h,0,0)$ depending on the orientation of the nickel crystal. Corrections were made for the deadtime of the detector.

The low-order nickel reflections were not measured in this experiment for two reasons: (i) they had been studied by Zukowski *et al.* (1992) and (ii) this investigation was made as part of the commissioning of the optics hutch at a time when a long air path was unavoidable. This meant that these low-energy reflections were in any case severely attenuated in air. Other details of the measurement technique have been reported by Zukowski *et al.* (1992).

3. Results

3.1. Beam polarization

For a single electron, the synchrotron radiation flux and polarization may be calculated using standard formulae (Schwinger, 1949). In a real electron beam containing many electrons there will be a range of electron trajectories such that at any point in the orbit the beam has a finite size and a range of velocities. It has been shown by Laundy (1990) that the modification to the formulae describing the emitted synchrotron radiation can be accomplished by the introduction of a single parameter, σ_γ , which characterizes the distribution of electron trajectories at a given point in the orbit.

In this experiment σ_γ was determined by measuring the Bragg intensity, $I(\varphi, \sigma_\gamma)$, as a function of the angle above, and below, the orbital plane for four of the strongest diffraction peaks,

$$I(\varphi, \sigma_\gamma) = A[1 - P_L(\varphi, \sigma_\gamma)]I(\varphi, \sigma_\gamma), \quad (5)$$

where A is a constant for a given reflection and φ is the azimuthal angle. The functions $P_L(\varphi, \sigma_\gamma)$ and $I(\varphi, \sigma_\gamma)$ involve Bessel functions (for details, see Laundy, 1990). The X-ray linear polarization, P_L , peaks close to unity on the beam orbit, *i.e.* when $\varphi = 0$, and hence the Bragg intensity is at a minimum. This locates accurately the beam centre. The sharpness of the minima depends strongly on σ_γ which can therefore be determined to a high degree of accuracy by fitting $I(\varphi, \sigma_\gamma)$ to the measured Bragg intensity with A and σ_γ as variables. We found $\sigma_\gamma = 33.4 \pm 0.6$ nrad. From this result, P_L and P_C , together with their angle and energy dependence, can be determined from the formulae developed by Laundy (1990).

The linear polarization is shown in Fig. 1(a) for an angular range of $6 \mu\text{rad}$ above and below the orbital plane and a photon energy of 10 keV which is close to the critical energy of the dipole magnet source. Its calculated value is 99.85 (1)% at the beam centre. The corresponding value at 5 keV is 99.88 (1)% and at 15 keV it is 99.83 (1)%. The high precision of this result arises because it is essentially $1 - P_L(\varphi, \sigma_\gamma)$ that is measured and consequently the random error in P_L is no more than $\pm 0.01\%$. The value is dependent on the electron beam parameters which determine σ_γ . At the ESRF these are specified to remain within $\pm 10\%$ of their nominal value. The corresponding change in the linear polarization, P_L , on orbit is only $\pm 0.01\%$. The extremely high degree of linear polarization determined here is crucial in magnetic form factor measurements. Fig. 1 also shows the angular variation of P_C and the factor $f_P = P_C/(1 - P_L)$ which enhances the ratio of magnetic to charge form factors in (4).

3.2. Magnetic form factor

The original analysis of neutron measurements of the magnetic form factor of nickel (Mook, 1966) used a model in which the magnetization density is derived from a free-ion Ni^{++} density plus a delocalized reverse-polarized $4s$ spin density. The Ni $3d$ orbitals are split by the cubic crystalline field into triply degenerate, t_{2g} , and doubly degenerate, e_g , orbitals. The occupancy ratio, r , of e_g to t_{2g} orbitals determines the degree of asphericity of the $3d$ charge cloud. When $r = 2/5$, the d orbitals are spherically symmetric. The total magnetic form factor, $f^{\text{mag}}(\mathbf{K})$, can be expressed in terms of the $3d$ spin form factor, $f^S(\mathbf{K})$, the $3d$ orbital form factor, $f^L(\mathbf{K})$, and the magnetic form factor produced by polarization of the core electrons, $f^{\text{core}}(\mathbf{K})$. In this treatment we use form factors which are normalized at $|\mathbf{K}| = 0$ to the total magnetic moment as opposed to the unitary neutron form factors which are normalized to unity at $\mathbf{K} = 0$,

Table 1

X-ray magnetic form factor of nickel.

The calculated values are based on the Hartree–Fock wave functions of Watson & Freeman (1960*a,b*).

Reflection (<i>hkl</i>)	$\sin \theta/\lambda$ (\AA^{-1})	Experiment		$f(\mathbf{K})$	Calculation	
		$f^{\text{mag}}(\mathbf{K})/f(\mathbf{K})$ (%)	$f^{\text{mag}}(\mathbf{K})$		$f^{\text{core}}(\mathbf{K})$	$f^{\text{mag}}(\mathbf{K})$
440	0.803	+0.31 (6)	+0.025 (5)	8.211	−0.0027	+0.0279
600	0.851	−0.19 (3)	−0.018 (3)	7.809	−0.0030	−0.0173
800	1.135	−0.46 (1)	−0.035 (1)	6.313	−0.0040	−0.0335
660	1.204	−0.07 (2)	−0.004 (1)	6.057	−0.0041	−0.0038
1000	1.419	−0.41 (1)	−0.027 (1)	5.332	−0.0041	−0.0284
880	1.605	−0.10 (2)	−0.005 (1)	4.735	−0.0038	−0.0051
1200	1.703	−0.36 (2)	−0.019 (1)	4.432	−0.0036	−0.0206
1400	1.985	−0.26 (8)	−0.012 (3)	3.609	−0.0029	−0.0140
1600	2.270	−0.15 (7)	−0.005 (3)	2.922	−0.0021	−0.0093
1800	2.554	−0.19 (7)	−0.005 (2)	2.390	−0.0015	−0.0060

$$f^{\text{mag}}(\mathbf{K}) = 1 + \alpha[1 - \delta(\mathbf{K})]f^S(\mathbf{K}) + f^L(\mathbf{K}) + f^{\text{core}}(\mathbf{K}), \quad (6)$$

where the delta function, $\delta(\mathbf{K})$, insures that the uniform 4s density only contributes at $\mathbf{K} = 0$; the fraction of the total moment derived from the reverse polarized spin density is represented by the parameter α .

Weiss & Freeman (1958) showed that the form factor can be written in terms of integrals of the form

$$\langle j_n \rangle_{ij} = \int_0^\infty U_i(r)U_j(r)j_n(Kr)dr, \quad (7)$$

where $K = 4\pi \sin \theta/\lambda$, $U_i(r)$ is the radial part of the wave function for the i th orbital and $j_n(Kr)$ are the n th-order spherical Bessel functions. The ratio of the spin to orbital moments is determined by the spectroscopic splitting factor, g , which in nickel is 2.2 (Scott, 1962). The 3d spin and orbital form factor can be written as

$$f^S(\mathbf{K}) = [\langle j_0 \rangle + A_{hkl}(5r/2 - 1)\langle j_4 \rangle]2\mu/g, \quad (8)$$

$$f^L(\mathbf{K}) = (\langle j_0 \rangle + \langle j_2 \rangle)[(g - 2)/g]\mu, \quad (9)$$

where the factor A_{hkl} is a function of the Miller indices hkl ,

$$A_{hkl} = \frac{h^4 + k^4 + l^4 - 3(h^2k^2 + h^2l^2 + k^2l^2)}{(h^2 + k^2 + l^2)^2}. \quad (10)$$

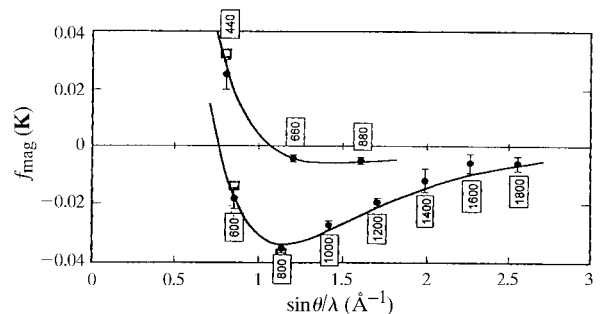
In the white-beam X-ray method it is possible to measure reflections to higher order than with neutrons for two reasons. First, the X-ray cross section for magnetic scattering is proportional to the photon energy, which in the energy-dispersive method increases with the momentum transfer $|\mathbf{K}|$. Second, the experiment measures the ratio of the magnetic to charge form factors. Although both decrease with K , their ratio decreases less rapidly than the absolute value of either. The highest-order X-ray reflections studied here are at $|\mathbf{K}| > 2.5 \text{\AA}^{-1}$ whereas the reflections measured using neutrons all fall below 1.2\AA^{-1} . The Ni charge form factor was calculated in the high- \mathbf{K} regime by taking Ni^{++} radial wave functions published by Watson & Freeman (1960*a,b*) and transforming them to give $f(\mathbf{K})$, $f^{\text{mag}}(\mathbf{K})$ and $f^{\text{core}}(\mathbf{K})$. To calculate $f(\mathbf{K})$ and $f^{\text{core}}(\mathbf{K})$, the symmetric $\langle j_o \rangle_{ii}$ term was summed over the appropriate orbitals, while, for the 3d magnetic contribution, equations

(6), (8) and (9) were used. We took $g = 2.2$, $\gamma = 0.19$ and $a = 0.19$ from Mook's analysis (Mook, 1966) of the neutron data. The experimental data and calculated values are summarized in Table 1, and are compared in Fig. 2. As can be seen, the agreement between the calculated and measured magnetic form factors is excellent over the entire wavevector range. The graph includes three low-order form factors from the neutron study: they are in good agreement with these X-ray data.

4. Conclusions

The degree of polarization of the ESRF dipole source on the XMaS beamline varies between 99.88 (1) and 99.83 (1)% between 5 and 15 keV, respectively. These values demonstrate that it is an excellent source for studies of ferromagnetism.

The experimental data fit the calculated magnetic form factor within experimental error and are therefore consistent with the interpretation of magnetization density in nickel given by Mook (1966). While there are still some questions over the validity of the form-factor fitting method (see, for example, Van Laar *et al.*, 1982), it is interesting that

**Figure 2**

Measured and calculated magnetic form factors for nickel at large momentum-transfer K . The filled black circles with error bars are the experimental values and lines represent the values predicted from the radial wave functions of Watson & Freeman (1960*a,b*). Three neutron results are available for comparison, at low momentum transfer values; they are shown by open squares and are taken from Mook (1966).

for these high-order reflections in nickel, which have not previously been measured, the X-ray data support the asphericity of the charge density with 19% of the 3d electrons in e_g and 81% in t_{2g} orbitals. They are also consistent with a *negatively* polarized component of the spin density amounting to 19% of the 3d moment, although these high-order reflections are less sensitive to this delocalized contribution than, for example, magnetic Compton scattering studies. The core polarization is significant for these high-order reflections although the 3d magnetic form factor is still dominant in this momentum transfer range.

The authors are grateful to the EPSRC for funding the XMaS construction-phase project; these measurements formed part of the commissioning process. We thank the CLRC Daresbury Laboratory for the loan of equipment. The study also formed part of a programme supported by the European Union under Contact ERCBCHRX CT 930135. We are grateful to M. Hart, J. B. Forsyth and P. J. Brown for invaluable guidance and advice.

References

- Blume, M. (1985). *J. Appl. Phys.* **57**, 3615–3618.
- Collins, S. P., Laundy, D. & Rollason, A. J. (1992). *Philos. Mag.* **B65**, 37–46.
- Laundy, D. (1990). *Nucl. Instrum. Methods*, **A290**, 248–253.
- Laundy, D., Collins, S. P. & Rollason, A. J. (1991). *J. Phys. Condens. Matter*, **3**, 369–375.
- Lovesey, S. W. (1987). *J. Phys. C*, **34**, 5625–5639.
- Lovesey, S. W. & Collins, S. P. (1996). *X-ray Scattering and Absorption by Magnetic Materials*. Oxford University Press.
- Mook, H. A. (1966). *Phys. Rev.* **148**, 495–501.
- Schwinger, J. (1949). *Phys. Rev.* **75**, 1912–1925.
- Scott, G. G. (1962). *J. Phys. Soc. Jpn Suppl.* **7(B)**, 372–375.
- Shull, C. G. & Yamada, Y. (1962). *J. Phys. Soc. Jpn Suppl.* **7(8)**, 1–11.
- Van Laar, B., Maniawski, F. & Kaprzyk, S. (1982). *J. Phys. C*, **7**, 113–118.
- Watson, R. E. & Freeman, A. J. (1960a). *Phys. Rev.* **120**, 1125–1134.
- Watson, R. E. & Freeman, A. J. (1960b). *Phys. Rev.* **120**, 1134–1141.
- Weiss, R. J. & Freeman, A. J. (1958). *J. Phys. Chem. Solids*, **10**, 147–161.
- Zukowski, E., Cooper, M. J., Armstrong, R., Ito, M., Collins, S. P., Laundy, D. & Andrejczuk, A. J. (1992). *J. X-ray Sci. Technol.* **3**, 300–310.